









ESTIMATING THE AVERAGE SIZE OF FIBER/MATRIX INTERFACE CRACKS IN UD AND CROSS-PLY LAMINATES

L. Di Stasio^{1,2}, J. Varna¹, Z. Ayadi²

¹ Division of Materials Science, Luleå University of Technology, Luleå, Sweden
² EEIGM & IJL, Université de Lorraine, Nancy, France

7th ECCOMAS Thematic Conference on the Mechanical Response of Composites











Outline

- Transverse Cracks Initiation in FRPC
- **Modeling**
- Debond Initiation
- Debond Propagation
- Conclusions











TRANSVERSE CRACKS INITIATION IN FRPC



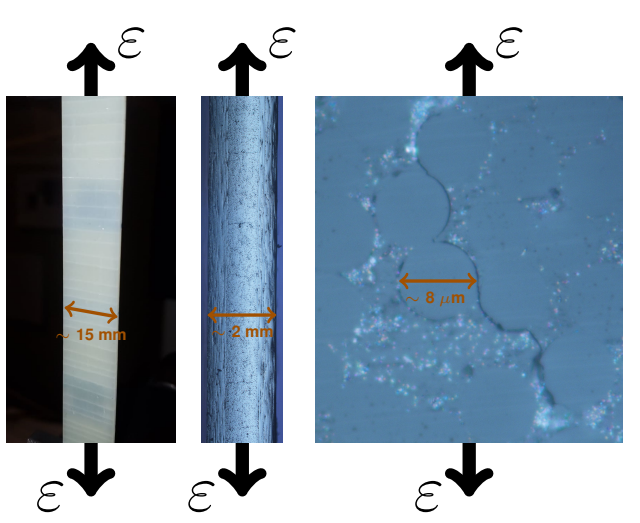








Micromechanics of Initiation: Transverse Tensile Loading



Left:

front view of $[0, 90_2]_S$, visual inspection.

Center:

edge view of [0, 90]_S, optical microscope.

Right:

edge view of $[0, 90]_S$, optical microscope.





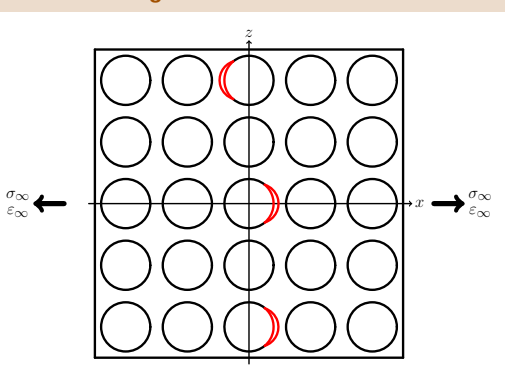






Micromechanics of Initiation: Transverse Tensile Loading

Stage 1: isolated debonds







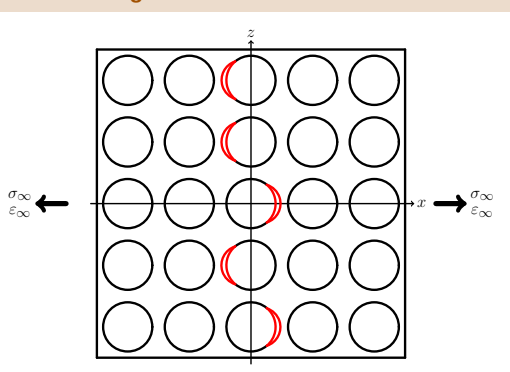






Micromechanics of Initiation: Transverse Tensile Loading

Stage 2: consecutive debonds







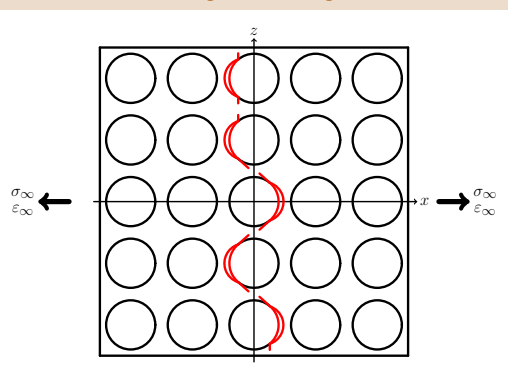






Micromechanics of Initiation: Transverse Tensile Loading

Stage 3: kinking







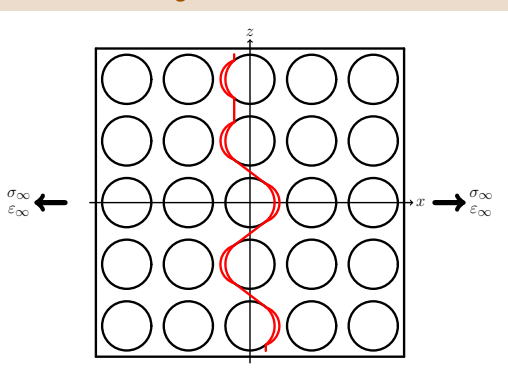






Micromechanics of Initiation: Transverse Tensile Loading

Stage 4: coalescence











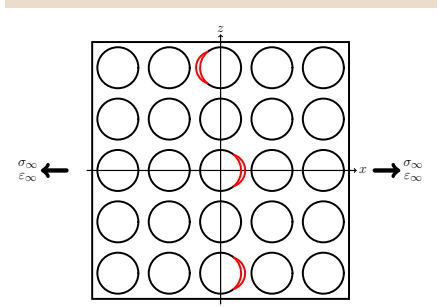




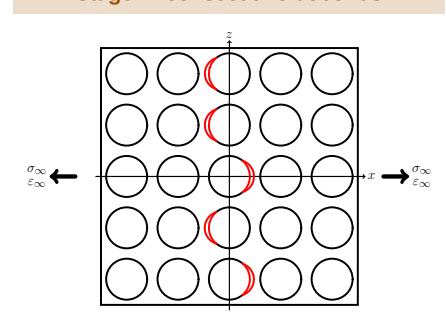
Objective of the Study

Can we talk about a ply-thickness effect for the fiber-matrix interface crack?

Stage 1: isolated debonds



Stage 2: consecutive debonds













Geometry Representative Volume Elements Assumptions Solution







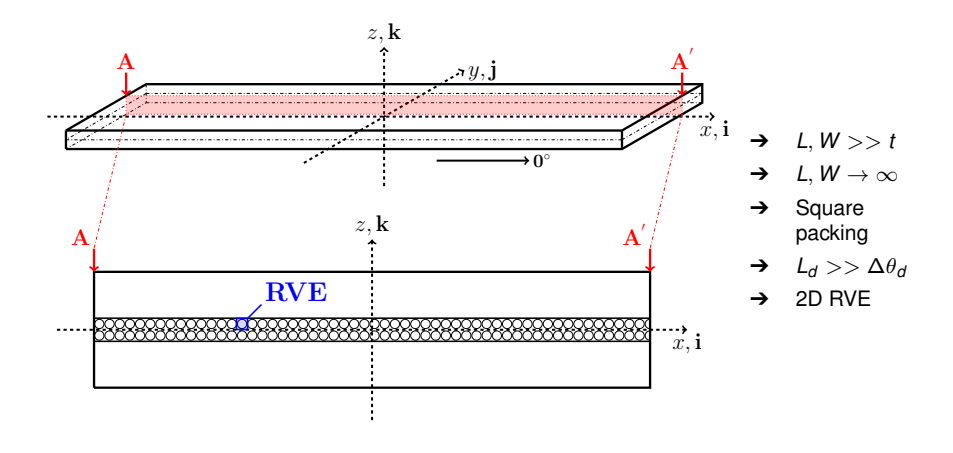






Transverse Cracks Initiation in FRPC Modeling Debond Initiation Debond Propagation Conclusions Geometry Representative Volume Elements Assumptions Solution

Geometry







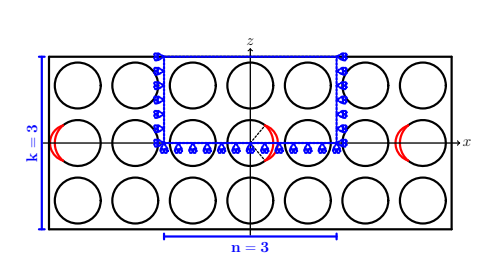




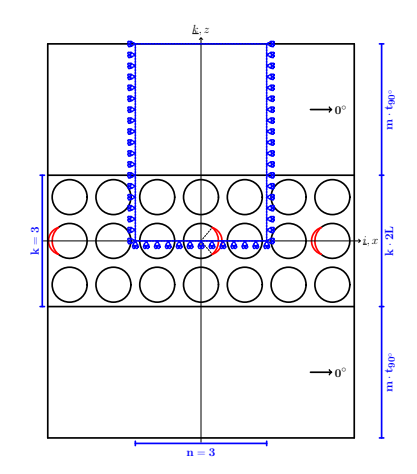


Transverse Cracks Initiation in FRPC Modeling Debond Initiation Debond Propagation Conclusions Geometry Representative Volume Elements Assumptions Solution

Representative Volume Elements



 $n \times k$ – free



$$n \times k - m \cdot t_{90^{\circ}}$$









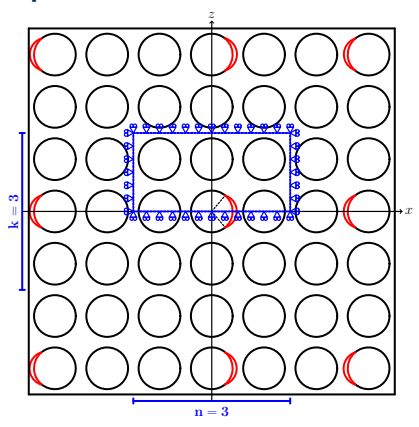
Conclusions



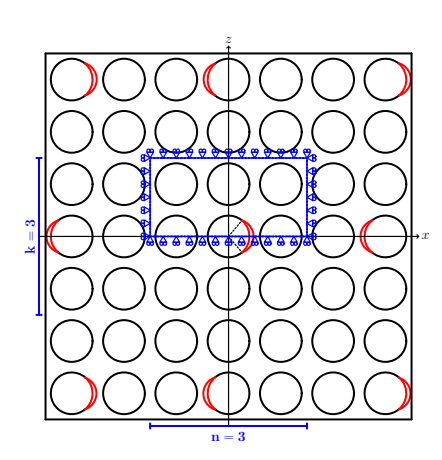
Transverse Cracks Initiation in FRPC Modeling Debond Initiation Debond Propagation

Geometry Representative Volume Elements Assumptions Solution

Representative Volume Elements



$$n \times k - symm$$



 $n \times k$ – asymm





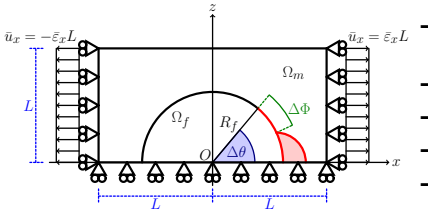






Transverse Cracks Initiation in FRPC Modeling Debond Initiation Debond Propagation Conclusions Geometry Representative Volume Elements Assumptions Solution

Assumptions



$$R_f = 1 \ [\mu m] \quad L = \frac{R_f}{2} \sqrt{\frac{\pi}{V_f}}$$

- Linear elastic, homogeneous materials
- Concentric Cylinders Assembly with Self-Consistent Shear Model for UD
- Plane strain
- Frictionless contact interaction
- Symmetric w.r.t. x-axis
- Coupling of x-displacements on left and right side (repeating unit cell)
- \rightarrow Applied uniaxial tensile strain $\bar{\varepsilon}_{x} = 1\%$
- → $V_f = 60\%$

Material	<i>V_f</i> [%]	E_L [GPa]	E_T [GPa]	μ_{LT} [GPa]	$ u_{LT}\left[- ight]$	$ u_{TT}\left[- ight]$
Glass fiber Epoxy	-	70.0 3.5	70.0 3.5	29.2 1.25	0.2 0.4	0.2 0.4
UD	60.0	43.442	13.714	4.315	0.273	0.465





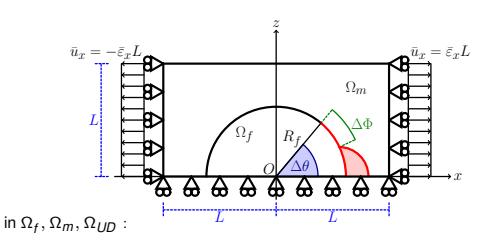






Transverse Cracks Initiation in FRPC **Modeling** Debond Initiation Debond Propagation Conclusions Geometry Representative Volume Elements Assumptions **Solution**

Solution



$$\begin{split} \frac{\partial^{2} \varepsilon_{XX}}{\partial z^{2}} + \frac{\partial^{2} \varepsilon_{ZZ}}{\partial x^{2}} &= \frac{\partial^{2} \gamma_{ZX}}{\partial x \partial z} & \text{for } 0^{\circ} \leq \alpha \leq \Delta \theta, \Delta \theta \neq 0^{\circ} : \\ \frac{\partial z}{\partial x} &= \frac{\partial z}{\partial x \partial z} & (\overrightarrow{U}_{m} (R_{f}, \alpha) - \overrightarrow{U}_{f} (R_{f}, \alpha)) \cdot \overrightarrow{n}_{\alpha} \geq 0 \\ \varepsilon_{y} &= \gamma_{xy} = \gamma_{yz} = 0 & \text{for } \Delta \theta \leq \alpha \leq 180^{\circ} : \\ \frac{\partial \sigma_{XX}}{\partial x} + \frac{\partial \tau_{ZX}}{\partial z} &= 0 & \overrightarrow{U}_{m} (R_{f}, \alpha) - \overrightarrow{U}_{f} (R_{f}, \alpha) = 0 \\ \frac{\partial \tau_{ZX}}{\partial x} + \frac{\partial \sigma_{ZZ}}{\partial z} &= 0 & \tau_{ij} = E_{ijkl} \varepsilon_{kl} \\ \frac{\partial z}{\partial x} &= \nu \left(\sigma_{YX} + \sigma_{ZZ}\right) \end{split}$$

 $\forall \Delta \theta \neq 0^{\circ}$

oscillating singularity

$$\sigma \sim r^{-\frac{1}{2}} \sin(\varepsilon \log r), \quad V_f \to 0$$

$$\varepsilon = \frac{1}{2\pi} \log \left(\frac{1-\beta}{1+\beta} \right)$$

$$\beta = \frac{\mu_2 (\kappa_1 - 1) - \mu_1 (\kappa_2 - 1)}{\mu_2 (\kappa_1 + 1) + \mu_4 (\kappa_2 + 1)}$$

→ receding contact

$$\Rightarrow \quad \frac{G(R_{f,2})}{G(R_{f,1})} = \frac{R_{f,2}}{R_{f,1}}, \frac{G(\bar{\varepsilon}_{x,2})}{G(\bar{\varepsilon}_{x,1})} = \frac{\bar{\varepsilon}_{x,2}^2}{\bar{\varepsilon}_{x,1}^2}$$

→ FEM + LEFM (VCCT)

regular mesh of quadrilaterals at the crack tip:

-
$$AR \sim 1$$
, $\delta = 0.05^{\circ}$ $\forall \Delta \theta$

→ 2nd order shape functions











 $\sigma_{
m rr}$ vs $au_{
m r heta}$ $\sigma_{
m LHS}$ $\sigma_{
m vM}$ $\sigma_{
m I}$ Observations & Conclusions







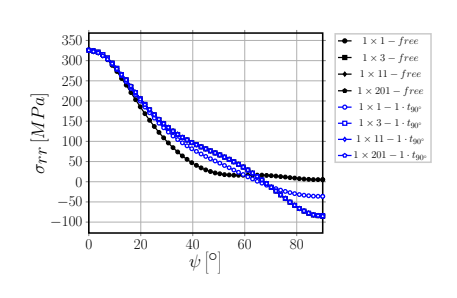


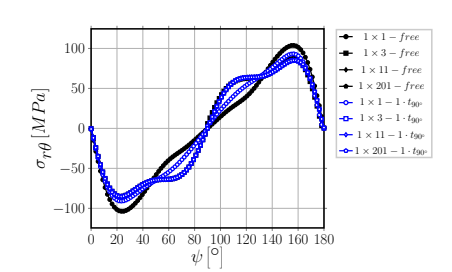


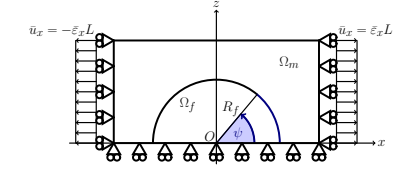


 σ_{rr} vs $\tau_{r\theta}$ σ_{IHS} σ_{vM} σ_{I} Observations & Conclusions

$\sigma_{\rm rr}$ vs $\tau_{\rm r heta}$: radial stress vs tangential shear at the interface











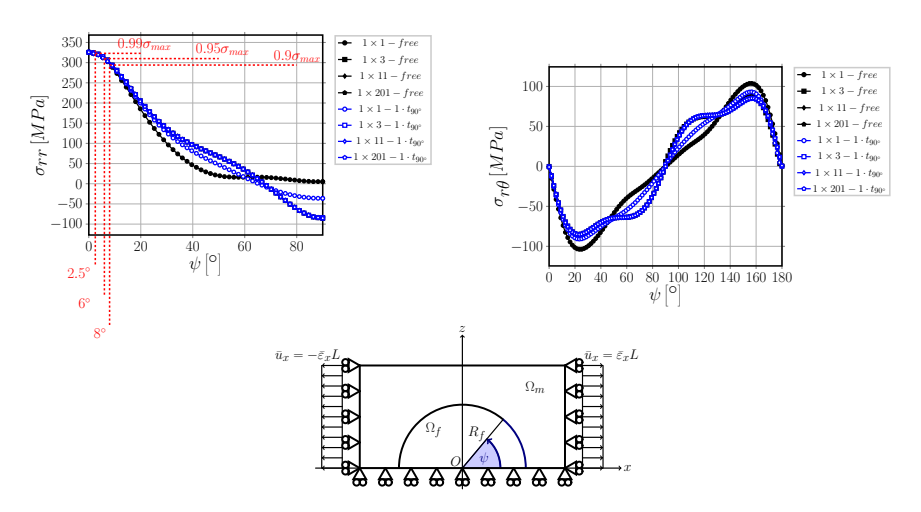






$au_{ extbf{rf}}$ vs $au_{ extbf{ extit{f}} heta}$ $\sigma_{ extit{LHS}}$ $\sigma_{ extit{VM}}$ $\sigma_{ extit{I}}$ Observations & Conclusions

$\sigma_{\rm rr}$ vs $\tau_{\rm r\theta}$: radial stress vs tangential shear at the interface







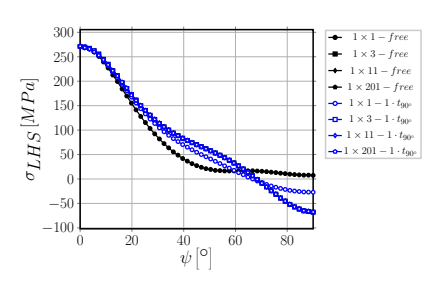


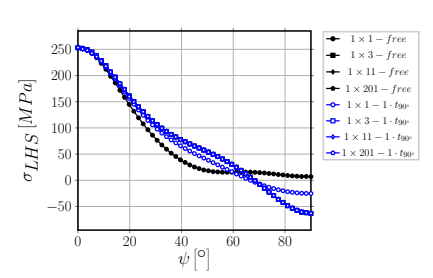


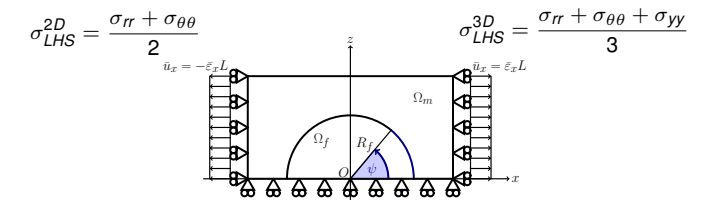


Observations & Conclusions

σ_{LHS} : local hydrostatic stress at the interface











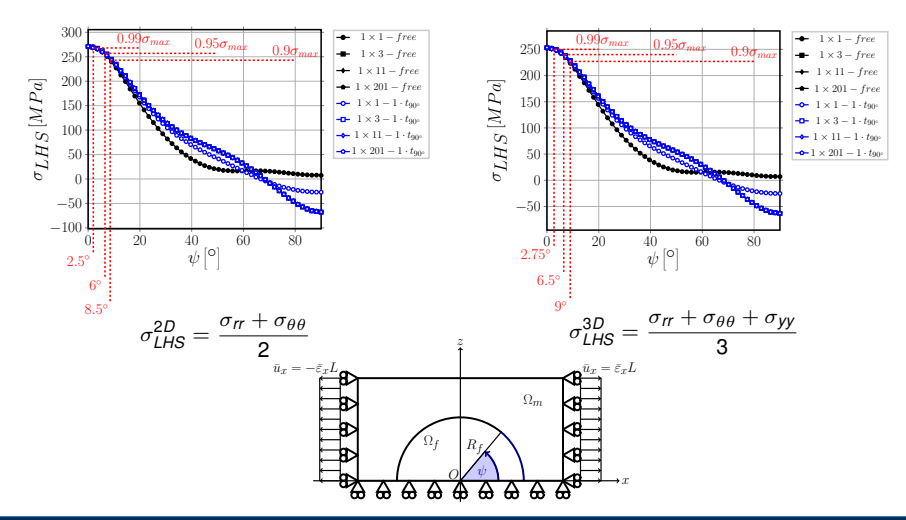






 σ_{rr} vs $\tau_{r\theta}$ σ_{IHS} σ_{vM} σ_{I} Observations & Conclusions

σ_{LHS} : local hydrostatic stress at the interface









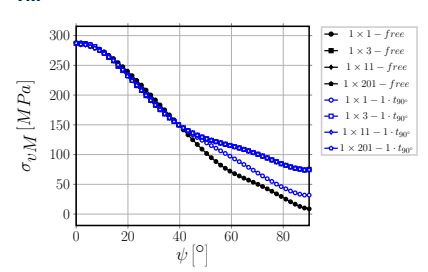


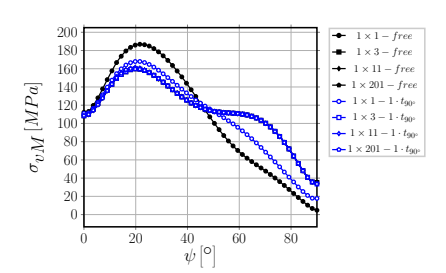


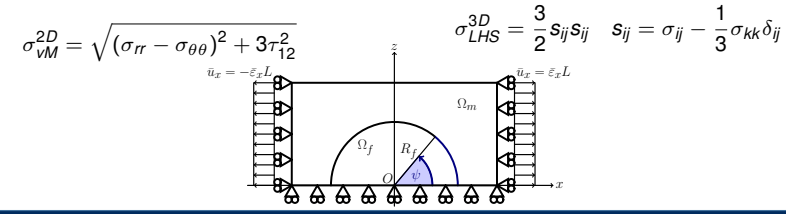
Debond Initiation Debond Propagation Transverse Cracks Initiation in FRPC Modeling Conclusions

Observations & Conclusions

σ_{vM} : von Mises stress at the interface











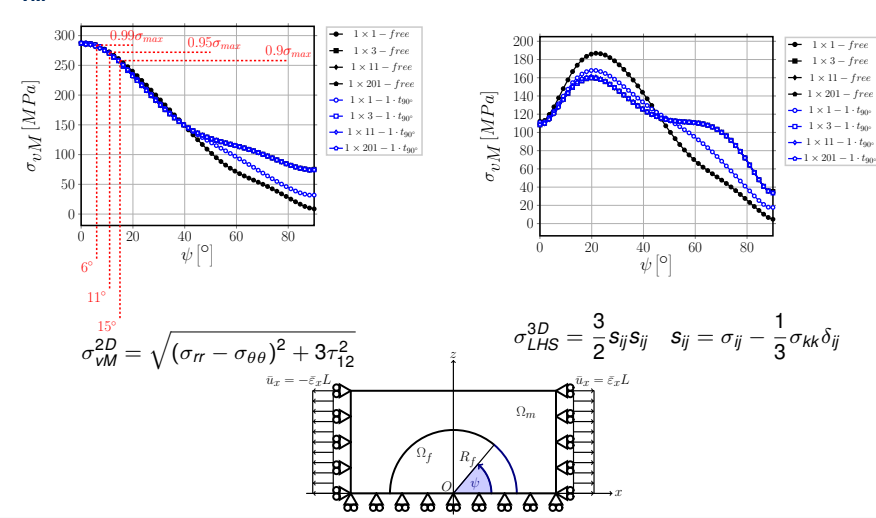






Observations & Conclusions

σ_{vM} : von Mises stress at the interface







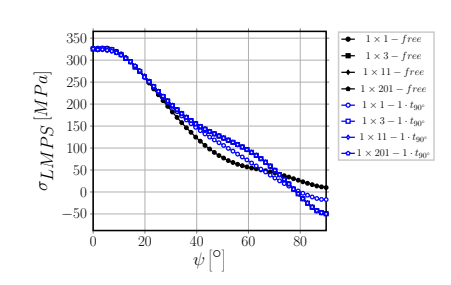


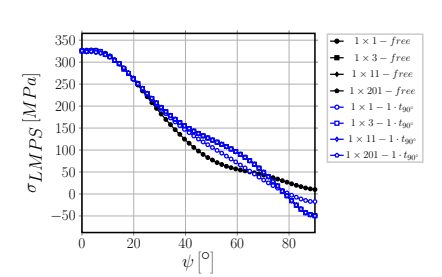


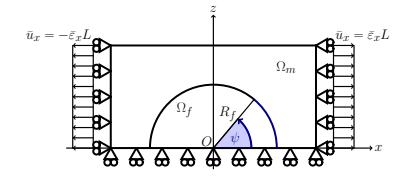


 $\sigma_{
m rr}$ vs $au_{
m r heta}$ σ_{IHS} σ_{VM} σ_{I} Observations & Conclusions

$\sigma_{\rm I}$: maximum principal stress at the interface











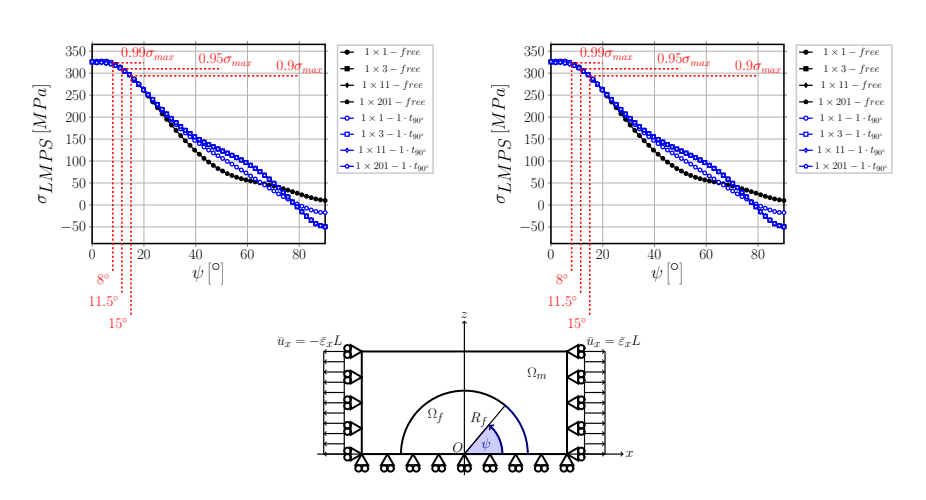






 $\sigma_{
m rr}$ vs $au_{
m r heta}$ σ_{IHS} σ_{vM} σ_{I} Observations & Conclusions

σ_l : maximum principal stress at the interface













 σ_{rr} vs τ_{rA} σ_{IHS} σ_{vM} σ_{I} Observations & Conclusions

Observations & Conclusions

- For all stresses analyzed, no significant difference is present between the different RUCs for $\psi < 10^{\circ}$:
- \rightarrow for all stresses analyzed, no difference can be observed by increasing k when $k \geq 3$;
- ⇒ for all stresses analyzed, no difference can be observed between $1 \times k$ free and $1 \times k 1 \cdot t_{00^\circ}$ for k > 3;
- → σ_{rr}, σ_{LHS,2D}, σ_{LHS,3D}, σ_{νM,2D}, σ_{LMPS,2D} and σ_{LMPS,3D} all reach their peak value at 0° and 180° and decrease to 99% the peak value between 2° and 8°, to 95% the peak value between 6° and 12° and to 90% the peak value between 8° and 15° from the occurrence of the maximum.

It seems reasonable to conclude that...

...a stress-based criterion would predict, irrespectively of the specific criterion chosen, the onset of an interface crack at 0° or 180° with an initial size at least comprised in the range $2^{\circ} - 8^{\circ}$ (1% margin) and likely in the range $6^{\circ} - 12^{\circ}$ (5% margin).











stimation of G_{lc} Estimation of $\Delta heta_{max}$ Observations & Conclusion







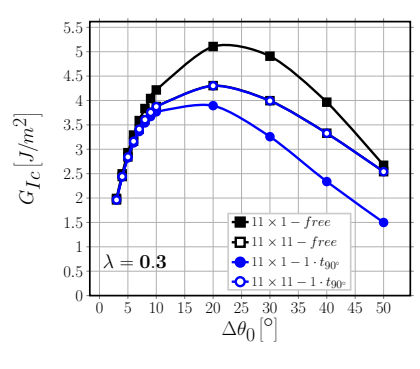


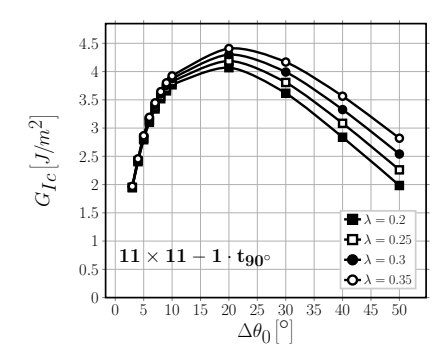




Estimation of G_{lc} Estimation of $\Delta \theta_{max}$ Observations & Conclusions

Estimation of G_{lc}





$$G_{lc} = \left. rac{G_c}{1 + an^2\left(\left(1 - \lambda
ight)\Psi_G
ight)} \right|_{G_c = G_{TOT}\left(\Delta heta_0
ight)}, \quad \Psi_G = an^{-1}\left(\sqrt{rac{G_{ll}}{G_l}}
ight) \right|_{\Delta l}$$

$$\Psi_G = tan^{-1} \left(\sqrt{\frac{G_{II}}{G_I}} \right) \bigg|_{\Delta\theta_I}$$







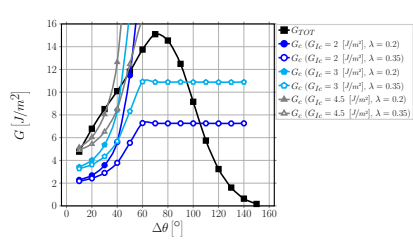




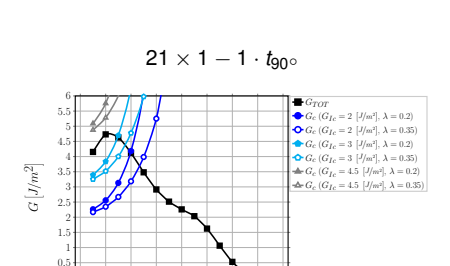
Estimation of $\Delta \theta_{max}$ Observations & Conclusions

Estimation of $\Delta \theta_{max}$





$$\Delta heta_{max} \in (30^\circ - 105^\circ)$$



Conclusions

$$\Delta \theta_{max} \in (30^{\circ} - 50^{\circ})$$

20 40 60 80 100 120 140

$$G_{TOT}\left(\Delta heta
ight) > G_{c} = G_{lc}\left(1 + an^{2}\left(\left(1 - \lambda
ight)\Psi_{G}
ight)
ight), \quad \Psi_{G} = \left. an^{-1}\left(\sqrt{rac{G_{ll}}{G_{l}}}
ight)
ight|_{\Delta heta}$$





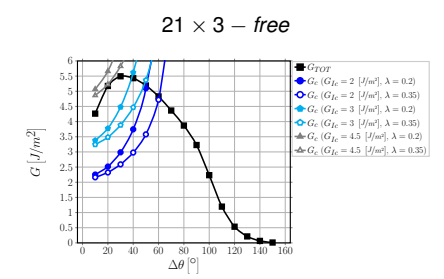






Estimation of G_{lc} Estimation of $\Delta \theta_{max}$ Observations & Conclusions

Estimation of $\Delta \theta_{max}$



 $21 \times 3 - 1 \cdot t_{900}$

Conclusions

$$\Delta \theta_{max} \in (40^{\circ} - 60^{\circ})$$

$$\Delta \theta_{max} \in (40^{\circ} - 60^{\circ})$$

$$G_{TOT}\left(\Delta heta
ight) > G_{c} = G_{lc}\left(1 + an^{2}\left(\left(1 - \lambda
ight)\Psi_{G}
ight)
ight), \quad \Psi_{G} = \left. an^{-1}\left(\sqrt{rac{G_{ll}}{G_{l}}}
ight)
ight|_{\Delta heta}$$







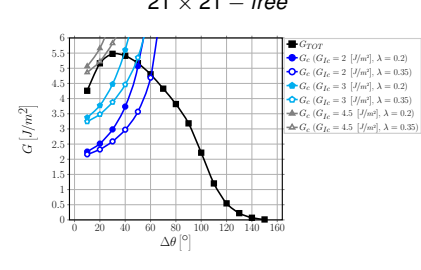




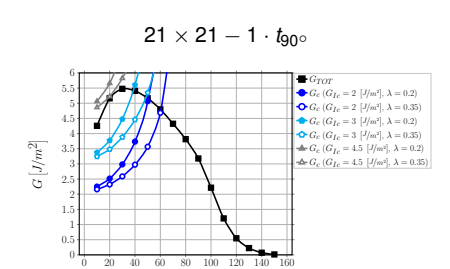
Transverse Cracks Initiation in FRPC Modeling Debond Initiation **Debond Propagation**Estimation of G_{lc} **Estimation of** $\Delta\theta_{max}$ **Observations & Conclusions**

Estimation of $\Delta \theta_{max}$

21 × 21 – free



$$\Delta \theta_{max} \in (40^{\circ} - 60^{\circ})$$



Conclusions

$$\Delta \theta_{max} \in (40^{\circ} - 60^{\circ})$$

$$G_{TOT}\left(\Delta heta
ight) > G_{c} = G_{lc}\left(1 + an^{2}\left(\left(1 - \lambda
ight)\Psi_{G}
ight)
ight), \quad \Psi_{G} = \left. an^{-1}\left(\sqrt{rac{G_{ll}}{G_{l}}}
ight)
ight|_{\Delta heta}$$







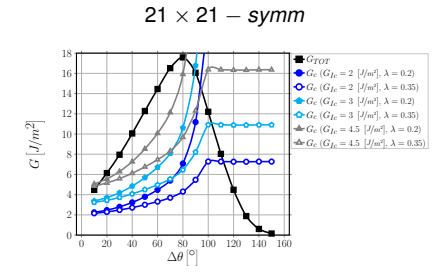




Conclusions

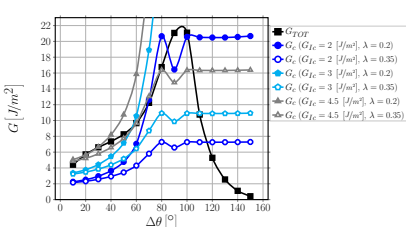
Estimation of G_{lc} Estimation of $\Delta \theta_{max}$ Observations & Conclusions

Estimation of $\Delta \theta_{max}$



$$\Delta \theta_{max} \in (80^{\circ} - 110^{\circ})$$

$21 \times 21 - asymm$ $-G_{TOT}$ 18 16



$$\Delta \theta_{max} \in (55^{\circ} - 115^{\circ})$$

$$G_{TOT}\left(\Delta heta
ight) > G_{c} = G_{lc}\left(1 + an^{2}\left(\left(1 - \lambda
ight)\Psi_{G}
ight)
ight), \quad \Psi_{G} = \left. an^{-1}\left(\sqrt{rac{G_{ll}}{G_{l}}}
ight)
ight|_{\Delta heta}$$











Transverse Cracks Initiation in FRPC Modeling Debond Initiation Debond Propagation Conclusions Estimation of G_{lc} Estimation of $\Delta\theta_{max}$ Observations & Conclusions

Observations & Conclusions

- → The effect of the presence of the 0° layer is to reduce the maximum size of debonds;
- → however, the estimated debond size is the same for n × k − free and n × k − 1 · t_{90°} for k > 3:
- → the presence of a debond on the neighboring fiber in the vertical direction (21 × 1 − coupling and 21 × 1 − asymm) favors instead the growth of larger debonds;
- → the largest size is achieved when debonds are on opposite sides of consecutive fibers.

Estimated debond size range in cross-ply ($n \times k - 1 \cdot t_{90^{\circ}}$)

 $40^{\circ} - 60^{\circ}$

Measured debond size range in cross-ply (Correa et al., Compos. Sci. Technol. 155 (213-220), 2018)

 $21.4^{\circ} - 89.2^{\circ}$, average 49.3° , standard deviation of 11.7° 63% of measurements in $40^{\circ} - 60^{\circ}$ range











Transverse Cracks Initiation in FRPC Modeling Debond Initiation

Debond Propagation

Conclusions



Conclusions











Transverse Cracks Initiation in FRPC Modeli

Debond Initiation

Debond Propagation

Conclusions

Conclusions

- A stress criterion for initiation would likely predict, irrespectively of which criterion from those proposed in the literature is chosen, the onset of a debond at 0° or 180° with a semi-aperture Δθ₀ in the range 2° 12°, corresponding to a margin of 5% on the satisfaction of the criterion.
- → Assuming that debond propagation occurs unstably immediately after debond onset at the same level of global applied strain \(\bar{\varepsilon}_{x}\), it is possible to evaluate the parameter \(G_{lc}\) in the expression of the critical ERR and with it to estimate the range of expected maximum debond size.
- → The prediction for a cross-ply laminate (models $n \times k 1 \cdot t_{90^{\circ}}$, $k \ge 3$) agrees well with the debond size distribution in $\begin{bmatrix} 0_3^{\circ}, 90_3^{\circ} \end{bmatrix}_S$ estimated in *Correa et al., Compos. Sci. Technol.* 155 (213-220), 2018 through microscopic observations.











ransverse Cracks Initiation in FRPC Modeli

Debond Initiation

Debond Propagation

Conclusions

Thank you for listening today!

